Hydrology and Earth System Sciences

Discussions

Open Access

Integrated assessment of global water scarcity over the 21st century – Part 2: Climate change mitigation policies

M. I. Hejazi[1], J. Edmonds[1], L. Clarke[1], P. Kyle[1], E. Davies[2], V. Chaturvedi[1], J. Eom[1], M. Wise[1], P. Patel[1], and K. Calvin[1]

[1]Joint Global Change Research Institute, Pacific Northwest National Laboratory, College Park, Maryland, USA
[2]Department of Civil and Environmental Engineering, University of Alberta, Alberta, Canada

Correspondence to: M. I. Hejazi (mohamad.hejazi@pnnl.gov)

HESSD

10, 3383–3425, 2013

Climate change mitigation policies

M. I. Hejazi et al.

Title Page

Abstract	Introduction
Conclusions	References
Tables	Figures

|◀ | ▶|
◀ | ▶

Back | Close

Full Screen / Esc

Printer-friendly Version

Interactive Discussion

Abstract

We investigate the effects of emission mitigation policies on water scarcity both glob-
ally and regionally using the Global Change Assessment Model (GCAM), a leading
community integrated assessment model of energy, agriculture, climate, and water.
Three climate policy scenarios with increasing mitigation stringency of 7.7, 5.5, and
4.2 W m^{-2} in year 2095 (equivalent to the SRES A2, B2, and B1 emission scenarios,
respectively), under two carbon tax regimes (a universal carbon tax (UCT) which in-
cludes land use change emissions, and a fossil fuel and industrial emissions carbon
tax (FFICT) which excludes land use change emissions) are analyzed. The results are
compared to a baseline scenario (i.e. no climate change mitigation policy) with radia-
tive forcing reaching 8.8 W m^{-2} (equivalent to the SRES A1Fi emission scenario) by
2095. When compared to the baseline scenario and maintaining the same baseline
socioeconomic assumptions, water scarcity declines under a UCT mitigation policy but
increases with a FFICT mitigation scenario by the year 2095 particularly with more
stringent climate mitigation targets. The decreasing trend with UCT policy stringency
is due to substitution from more water-intensive to less water-intensive choices in food
and energy production, and in land use. Under the FFICT scenario, water scarcity is
projected to increase driven by higher water demands for bio-energy crops. This study
implies an increasingly prominent role for water availability in future human decisions,
and highlights the importance of including water in integrated assessment of global
change. Future research will be directed at incorporating water shortage feedbacks
in GCAM to better understand how such stresses will propagate across the various
human and natural systems in GCAM.

1 Introduction

Struggling to understand the implications of global climate change, society has devoted
considerable attention to assessing the potential consequences of climate change on

different human and Earth systems and to devising adaptation and mitigation policies to minimize any potentially dangerous anthropogenic consequences. To clarify the longer-term nature of connections between human and natural Earth systems, several high resolution, interdisciplinary global integrated assessment (IA) models have emerged

5 and contributed significantly to the Intergovernmental Panel on Climate Change (IPCC) climate change assessment reports. IA models currently focus on energy, agriculture, land use, and climate. However, all assessments to date have implicitly assumed that emissions mitigation and adaptation to climate change will be unaffected by water scarcity – yet water availability may pose a significant constraint on our ability to adapt

10 to or mitigate climate change. As an example, global emission mitigation policies can significantly alter land use patterns, both by limiting land use change emissions, and by increasing bioenergy production. The future of bioenergy crops, an important component of many technology strategies to reduce greenhouse gas emissions, may depend critically on water (Brendes, 2008; Varghese, 2007; Gerbens-Leenes et al., 2009;

15 Berndes, 2002). Thus, water availability could impose severe limitations on both emissions mitigation and climate adaptation, making the ability to assess the implications of changing supplies and demands for water – stemming from a simultaneously evolving human population, economic system, technology, and climate – an important scientific development.

20 With rapid shifts to socioeconomic systems, especially in the developing world, and potentially large-scale but varying impacts of climate change on global and regional hydrological cycles occurring simultaneously, an integrated assessment framework is expected to provide rich insights into alternative future global water demand and supply scenarios. Thus, any quantification of climate change impacts on water scarcity is

25 incomplete without accounting for changes in both water availability and demands for humans. Several studies have assessed the impact of climate change on hydrology and water availability with a general consensus of runoff increasing in higher latitudes and decreases in arid and semiarid regions with more frequent extremes due to an enhanced water cycle through warming (Milly et al., 2005). Yet, much uncertainty remains

especially with regard to GCM simulations used to force the hydrologic system due the large differences in rainfall predictions.

Several global water management models coupled with global hydrologic models are also capable of producing water use estimates generally categorized in domestic, industrial, and agricultural sectors. However, there is potentially an infinite number of underlying assumptions that can replicate a particular emission scenario but induce vastly or somewhat different water demand projections. Future global water use estimates are generally driven by socioeconomic and technological change assumptions that reflect the storyline of the emission scenario producing the GCM climatic forcings (Alcamo et al., 2003; Shen et al., 2008; Vörösmarty et al., 2000; Arnell, 2004) or by a set of assumptions representing a wide range of socioeconomic pathways (Hejazi et al., 2013b). However, future water demands can be affected by climate change mitigation policies (i.e. policies designed to reduce emissions of greenhouse gases, GHGs), which could feed back to affect the land and energy systems, and subsequently global water supply and demands (Falkenmark, 1999; Vörösmarty et al., 2000; Jackson et al., 2001). In this paper, we quantify the effect of various climate change mitigation policies on global and regional water demands and scarcity conditions.

Several authors have assessed water scarcity conditions both globally and regionally (Alcamo et al., 2003; Alcamo and Henrichs, 2002; Vörösmarty et al., 2000; Shen et al., 2008; Wada et al., 2011) with estimates of about one third of world population currently living in water scarce countries. However, fewer studies (Arnell, 2004; Arnell et al., 2011; Alcamo et al., 2007) have investigated the effect of climate change on water scarcity and only one study has investigated the implications of climate policy on global water scarcity (Arnell et al., 2011). Arnell et al. (2011) compares the percentage of the population living in scarce areas under a baseline scenario (no climate policy) and a climate mitigation of policy of 450 ppm CO_2e (equivalent carbon dioxide) by 2100. In this paper, we follow a similar approach by studying the effect of different types and levels of climate change mitigation policies. Instead of linking results from a set of models like Arnell et al.'s (2011) study – which used the IMAGE model and Shen

et al.'s (2008) water withdrawals – we use linked water demand and supply modules incorporated within an IA model to ensure consistency and the ability to pinpoint the system components responsible for any important observed changes. This capability can provide greater insight about the implications of climate policies on the dynamics of natural Earth systems and help to identify important technological investment and adaptation measures.

In the companion paper (Hejazi et al., 2013c), we incorporated water demand and supply modules in the global change assessment model (GCAM) under a baseline scenario that is equivalent to the radiative forcing of the A1Fi emission scenario ($8.8 \, \mathrm{W \, m^{-2}}$ by the end the century). In this paper, we investigate several scenarios that illustrate the effects of a set of human-induced climate change scenarios on water availability and demand, and consequently water scarcity both globally and regionally. More specifically, a set of climate change mitigation policies is simulated with the GCAM framework to investigate policy consequences of water scarcity. Climate policies following two different policy regimes and three different capping levels that are equivalent to the radiative forcing of the SRES A2, B2, and B1 emission scenarios (e.g. $7.2 \, \mathrm{W \, m^{-2}}$, $5.2 \, \mathrm{W \, m^{-2}}$, $4.2 \, \mathrm{W \, m^{-2}}$ in total GHG, respectively) are used to simulate the GCAM system. The two policy regimes are the Universal Carbon Tax (UCT) and the Fossil Fuel and Industrial emissions Carbon Tax (FFICT), which are intended to capture the level of uncertainty arising from the adopted climate change mitigation policies, especially with regard to energy choices and the level of bioenergy use in the future – the two regimes induce different production levels of bioenergy crops in the future among other differences in land use and energy choices. Thus, instead of exogenously assigning arbitrary amounts of bioenergy production over time, the climate policy mechanism projects bioenergy production based on an internally-consistent global integrated assessment model.

The main objectives of this paper are to quantify, in an integrated framework, the effects of climate mitigation policies on global and regional water scarcity estimates,

and to account for uncertainty arising from using different GCMs and following different types and constraining levels of climate policies on water scarcity.

2 GCAM overview

2.1 Overview

5 The Global Change Assessment Model (GCAM) has played a central role in the United States and international assessment process since its inception (Edmonds and Reilly, 1985; Clarke et al., 2007; Kim et al., 2006; Brenkert et al., 2003). GCAM is a dynamic-recursive model combining representations of the global economy, the energy system, agriculture and land use, climate, and recently added a water system (water demand
10 and water availability modules) (Hejazi et al., 2013b). The climate sub-model includes terrestrial and ocean carbon cycles, and a suite of coupled gas-cycle, climate, and ice-melt models. In its current implementation GCAM has the following 14 geopolitical regions: the United States, Canada, Western Europe, Japan, Australia and New Zealand, Former Soviet Union, Eastern Europe, Latin America, Africa, Middle East, China (and
15 Asian reforming economies), India, South Korea, and the rest of South and East Asia. GCAM establishes market-clearing prices for all energy, agriculture and land markets in each five-year time step from 2005 to 2095, such that supplies and demands for all markets are in equilibrium. In the current GCAM form, water does not hold any monetary value, and when demand exceeds the water availability, and additional supply is
20 assumed to come from non-renewable groundwater.

2.2 Water availability module

In the companion paper (Hejazi et al., 2013c), we present the global water availability model (GWAM) and explain its coupling with the existing GCAM systems, followed by a validation procedure to ensure the adequacy of the model to simulate average
25 annual runoff estimates at different spatial scales. GWAM is a gridded monthly water

balance model with 0.5 × 0.5 degrees. It requires gridded monthly precipitation, temperature, and maximum soil storage capacity (a function of land cover) and computes the amounts of evapotranspiration and evaporation to the atmosphere, runoff, and soil moisture in the soil column at the gridded monthly scale. GWAM is simulated over the entire 21st century usingthe SRES A1Fi, A2, B1, and B2 emission scenarios (SRES, 2000) and four GCMs (HadCM3, CSIRO2, CGCM2, PCM) (TYN SC 2.1 – Mitchell and Jones, 2005) to result in sixteen individual simulations of GWAM (four GCMs × four emission scenarios). In this study, we use the ensemble mean annual runoff of the four GCMs to establish the annual water availability in any grid cell for each of the four emission scenarios, i.e. the four GCMs are used individually to quantify the effect of GCM uncertainty on the water availability, and consequently, water scarcity. More details about the GWAM model can be found in Hejazi et al. (2013c).

2.3 Water demand module

GCAM representation of the water demand module consists of six major water demand sectors (Hejazi et al., 2013b, c), namely: domestic (Hejazi et al., 2013a), irrigation (Chaturvedi et al., 2012), livestock, electricity generation (Davies et al., 2012), primary energy production, and manufacturing. Some of the sectors include detailed representation of both subsectors and technologies (Hejazi et al., 2013b, c). These sectors are explicitly linked to the other existing GCAM systems (economy, energy, agricultural and land use, and climate). GCAM produces water demand projections at either the GCAM regional scale (fourteen regions globally) or the agro-ecological zone scale (151 AEZs globally). Results are then downscaled to the grid scale to match the spatial resolution of GWAM of $0.5° × 0.5°$ using proxy data with global coverage such as population density and livestock and crop maps along with areas equipped with irrigation as described in the companion paper (Hejazi et al., 2013c).

2.4 Water scarcity

Having estimates of both water availability and water demand projections in to the future at the same grid scale resolution, we compute water scarcity as the ratio of total water demand (withdrawal) over total amount of available water at each grid and basin on annual basis (Raskin et al., 1997). This definition of the water scarcity index (WSI) is sometimes referred to in the literature as the water resources vulnerability index (WRVI), the withdrawal-to-availability (WTA) ratio, and the criticality ratio (Brown and Matlock, 2011). Following previously suggested thresholds for water scarcity conditions (Falkenmark, 1999; Falkenmark et al., 2007), WSI is divided up into four categories: no scarcity (WSI < 0.1) low scarcity (0.1 ≤ WSI < 0.2), moderate scarcity (0.2 ≤ WSI < 0.4) and severe scarcity (WSI ≥ 0.4). To be consistent with the temporal and spatial scale of GWAM and following the adopted approach in the companion paper (Hejazi et al., 2013c), water demand (withdrawals) results are downscaled from the GCAM output scale (GCAM 14 regions, or 151 AEZ scale) to establish water scarcity for each grid cell and basin on a mean annual basis. Results reflecting the water scarcity estimates in years 200, 2050, and 2095 are average annual values corresponding to 1996–2002, 2046–2055, and 2091–2100 periods, respectively.

3 Policy scenarios

3.1 Baseline scenario (no climate policy)

To explore the consequences of climate change mitigation policies on water scarcity, we employ the same socioeconomic and technological change assumptions with both a set of policy scenarios and the baseline scenario. This permits isolation of human-induced climate change from population- and income-based effects on water scarcity. The baseline scenario is identical to the baseline scenario in the companion paper (Hejazi et al., 2013c), which reflects a world of fourteen billion people, slow technological

progress, high energy demands, and no climate policy. More specifically, going from year 2005 to year 2095, population increases from 6.5 billion to 13.7 billion, GDP increases from 30 trillion to 384 trillion (1990 US\$), and per capita GDP increases from 4607 to 28 136 (1990 US\$), while energy consumption globally increases from 458 EJ to 2236 EJ. This scenario is equivalent to the radiative forcing pathway associated with the SRES A1Fi scenario. The adopted SRES A1Fi scenario reflects an extreme scenario with no mitigation and is somewhat similar to the POP14/MDG-scenario in Hejazi et al. (2013b).

3.2 Climate change mitigation policy scenarios

In GCAM, policies designed to mitigate climate change are implemented in regions either as greenhouse gas emissions prices, or as constraints on greenhouse gas emissions, wherein the model solves for the emissions prices necessary to meet the constraints. These emissions policies may price terrestrial carbon dioxide emissions or they may not: Wise et al. (2009) uses two canonical carbon tax regimes, (1) a UCT regime which includes all carbon emissions in all sectors (including land use emissions) and all regions of the world; and (2) an FFICT regime which includes only fossil fuel and industrial emissions, but not land-use-related carbon emissions. Under both regimes, the carbon tax rises over time to limit atmospheric CO_2 concentrations to a prescribed stabilization level. However, the different types of policies lead to dramatically different outcomes for bioenergy deployment, land use change emissions, and consequently greenhouse gas emissions and climate change. The FFICT case is characterized by very high deployment of bioenergy and associated land use change emissions, which lead to greater emissions and climate change than the UCT case (Wise et al., 2009). However, in all previous results of various climate policy regimes and stabilization levels, water was never included as a potentially limiting resource for bioenergy production or any other activities. In this paper, with the assumption of unlimited non-renewable groundwater and no monetary value attached to water use in GCAM, we do not yet model the feedbacks that result when water demand exceeds

the regional water availability. Instead, we simply assess the impact of different target levels of climate change mitigation policies on water scarcity both globally and region-ally.

With radiative forcings producing climatic forcings that drive hydrology, one can match the adopted trajectory by either manipulating the socioeconomic and techno-logical change assumptions or by inducing a set of climate mitigation policies to cap emissions of GHGs to the atmosphere. In this study, we adopt the same socioeconomic and technological change assumptions as in the baseline scenario, and assume that climate change mitigation policies are used to adhere to the SRES radiative forcings trajectories by capping emissions.

GCAM is forced to match the radiative forcing associated with the SRES A1Fi emis-sion scenario. In GCAM, this emission pathway can be considered as a baseline sce-nario, wherein no climate change mitigation policy is considered. To investigate how different climate change mitigation policies could impact future water scarcity condi-tions, we have two means to ensure consistency between the selected climate policy and the corresponding GCM forcings used to simulate GWAM. One way is to spec-ify the emission or temperature change target – such as 450 parts per million (ppm) CO_2e or 2 °C by the end of the 21st century – and then to use a GCM run that re-flects the same radiative forcings trajectory as in GCAM. This can be a challenge since running a GCM or a set of GCMs to match every policy run can be computationally ex-pensive. One alternative is the use of downscaling techniques to match existing GCM runs to the pathway of interest, an approach that is typically adequate when perform-ing pattern-scaling on temperature but that has known deficiencies when applied to precipitation (Arnell et al., 2011; Cabré et al., 2010). A second alternative is to use existing GCM runs and then force GCAM to reproduce the equivalent radiative forc-ing trajectory through a particular climate policy. Given that the focus of the study is to explore the implications of climate change mitigation policies on water scarcity, we follow the latter approach in this paper. Thus, we devise climate policies in GCAM that reproduce the four SRES radiative forcings scenarios, where A1Fi is referred to as our

Title Page

Abstract   Introduction

Conclusions   References

Tables   Figures

◄   ►

Back   Close

Full Screen / Esc

Printer-friendly Version

Interactive Discussion

baseline scenario (no climate policy), and A2, B2, and B1 are three climate policy scenarios with increasing mitigation stringency of 7.7, 5.5, and 4.2 W m^{-2} in year 2095, respectively. Figure 1 shows the radiative forcing trajectories based on each of the four SRES emission scenarios (A1Fi, A2, B2, and B1) and each of the UCT and FFICT tax regimes to replicate SRES's emission pathways. Figure 2 shows the corresponding carbon price, CO_2 emission and concentration, and mean global temperature change associated with both the UCT and FFICT tax regimes and all four emission scenarios (A1Fi, A2, B2, and B1) when applicable. Note that the much lower reductions in emissions under the FFICT scenario, as compared to the UCT scenario, is a result of the energy portfolios of each policy regime, where FFICT typically results in a more pronounced contribution of bioenergy to energy than UCT. The A1Fi scenario (black solid line) reflects the no-climate policy scenario (baseline).

4   Results and discussion

4.1   Water availability

To reflect the effect of climate change on water availability, GWAM is simulated over the 21st century with four GCMs (PCM, CGCM2, CSIRO2, and HADCM3) and four emission scenarios (A1Fi, A2, B1, and B2), totaling sixteen simulations. The use of multiple GCMs facilitates the quantification of uncertainty associated with GCM results which feed in as input to GWAM. However, results are generally presented by considering their ensemble mean with equal weights. The four emission scenarios represent the baseline scenario and three climate policy scenarios with various levels of GHGs emission reduction targets. Figure 3 shows GWAM's simulations of global annual precipitation, actual evapotranspiration, and runoff from 1901–2100; future values are from the four GCMs and four emission scenarios. Globally, on land, the annual amounts of precipitation and actual evapotranspiration (ET) exhibit an upward trend for all the selected GCMs and emissions. However, only PCM and CSIRO2 exhibit an

upward trend in runoff as well while CGCM2 and HADCM3 show a slight decreasing trend in runoff. To understand the magnitude of potential shifts in water availability due to climate change and the level of variation from using different GCMs and emission scenarios, we compare annual precipitation, actual ET, and runoff estimates in years 2000, 2050, and 2095 (Fig. 4). These time periods are averaged over the 1996–2002, 2046–2055, and 2091–2100 periods, respectively, to filter out the year to year variations. Although each of the emission scenarios is associated with a particular warming level, the global amount of water availability does not show a consistent trend with temperature change across the GCM models. The level of uncertainty arising from employing different GCMs and emission scenarios increases over time, i.e. uncertainty is larger in 2095 than in 2050 (Fig. 4). Also, the uncertainty across GCMs is larger than across scenarios. Hence, averaging across GCMs to reflect a particular emission scenario reduces variability and results in a closer match to the historical average runoff, although spatial variations remain high in many cases. Figure 5 shows the difference in ensemble mean runoff at the grid scale between years 2095 and 2000 for each of the of four emission scenarios. Although globally humans may end up with more available water through runoff globally, when looking at the spatial distribution of gains and losses in freshwater, there are clear winners (Canada, Northern Europe, Russia, India, and northern China) and losers (e.g. most of South America, eastern half of the US, rest of Europe, the Middle East, and Southeast Asia and Australia). Those regional patterns are consistent across all four emission scenarios (as shown in Fig. 5), and somewhat similar to the finding of Arnell (2004), who found a reduction in runoff in much of Europe, the Middle East, southern Africa, North America and most of South America, and increasing runoff in high-latitude North America and Siberia, eastern Africa, parts of arid Saharan Africa and Australia, and South and East Asia.

4.2 Water demands

Global water demands (withdrawals and consumption) have been produced based on six climate policy scenarios (UCT7.7, UCT5.5, UCT4.2, FFICT7.7, FFICT5.5,

FFICT4.2). In all six policy scenarios, the global water withdrawals and consumption increase from the base-year level to the end of the century. Global water withdrawals increase in the baseline scenario from $3710\,\mathrm{km^3\,yr^{-1}}$ to $9062\,\mathrm{km^3\,yr^{-1}}$ by 2050 and $13\,318\,\mathrm{km^3\,yr^{-1}}$ by 2095. Global water consumptive use increase in the baseline scenario from $1215\,\mathrm{km^3\,yr^{-1}}$ to $3177\,\mathrm{km^3\,yr^{-1}}$ by 2050 and $4558\,\mathrm{km^3\,yr^{-1}}$ by 2095. Across all six climate policy scenarios, global water withdrawals range from $8843\,\mathrm{km^3\,yr^{-1}}$ in UCT4.2 to $9276\,\mathrm{km^3\,yr^{-1}}$ in FFICT4.2 in 2050 – and from $12\,533\,\mathrm{km^3\,yr^{-1}}$ in UCT4.2 to $25\,357\,\mathrm{km^3\,yr^{-1}}$ in FFICT4.2 in 2095. Similarly, global water consumptive use range from $3142\,\mathrm{km^3\,yr^{-1}}$ in UCT4.2 to $3350\,\mathrm{km^3\,yr^{-1}}$ in FFICT4.2 in 2050 – and from $4364\,\mathrm{km^3\,yr^{-1}}$ in UCT4.2 to $8719\,\mathrm{km^3\,yr^{-1}}$ in FFICT4.2 in 2095. In the remaining sections, the focus is on the quantity of water withdrawals even though both withdrawals and consumption are provided by GCAM.

Driven by increasing stringency in climate change mitigation policies and maintaining identical socioeconomic and technological assumptions across the six policy scenarios, Fig. 6 shows the global water withdrawals for the baseline and the six policy scenarios in comparison to historical estimates and forecasts. Gleick (2003) states that pre-1980 estimates of future projections tended to overestimate future global water withdrawals; however, our detailed, activity-based assessment of future water withdrawals generally yields higher future water withdrawals than those produced by recent studies (Alcamo et al., 2003; Shen et al., 2008), mainly due to high population projection associated with the baseline scenario in this study. Regardless, both previous studies and our scenarios indicate that water demands are likely to increase globally in this century, even in the most stringent future mitigation scenarios.

Figure 7 shows GCAM's estimates of global water demands (withdrawals) for the baseline scenario (no climate policy) and the six climate change mitigation policy scenarios for each of the water demand sectors; i.e. irrigation (biomass, crops), livestock, domestic, primary energy, electricity, and manufacturing. The variation in water demands by sector depends on the interdependence of each sector on the implications of the differing climate policy tax regimes (UCT vs. FFICT) and climate mitigations

Climate change mitigation policies

M. I. Hejazi et al.

Title Page

Abstract | Introduction

Conclusions | References

Tables | Figures

|◄ | ►|

◄ | ►

Back | Close

Full Screen / Esc

Printer-friendly Version

Interactive Discussion

targets. For example, biomass water withdrawals increase from zero in 2005 up to a range of 438–530 km^3 yr^{-1} in 2095 for the three UCT scenarios, and to a range of 1782–13 212 km^3 yr^{-1} in 2095 for the three FFICT scenarios. The large differences in the ranges are attributed to the dramatic increase of biomass production under the energy portfolio of the FFICT scenarios in meeting the climate policy targets. In contrast, municipal water demand shows no sensitivity to climate policy and all the six policy scenarios are identical to the baseline scenarios, i.e. from 466 km^3 yr^{-1} in 2005 to 1392 km^3 yr^{-1} in 2095; the effects of elevated temperatures on water demands are not accounted for in this study.

Total crop irrigation (excluding biomass) water withdrawals increase from 2464 km^3 yr^{-1} in 2005 to 9053–9686 km^3 yr^{-1} (UCT scenarios), and to 9078–9315 km^3 yr^{-1} (FFICT scenarios) in 2095. Livestock demands reflect the population- and income-driven growth in meat and dairy demands combined with a relatively minor price effect, increasing livestock water withdrawals from 18 km^3 yr^{-1} in 2005 to 39–54 km^3 yr^{-1} (UCT scenarios), and to 58–62 km^3 yr^{-1} (FFICT scenarios) in 2095. Domestic water withdrawals increase from 466 km^3 yr^{-1} (196 L person^{-1} day^{-1}) in 2005 to 1392 km^3 yr^{-1} (279 L person^{-1} day^{-1}) in 2095. Primary energy and electricity water demands could increase or decrease depending on the prevailing climate policy scenarios. Primary energy water withdrawals may increase (or decrease) from 19 km^3 yr^{-1} in 2005 to 34 km^3 yr^{-1} in baseline scenario due to higher coal and oil demands (or to 7 km^3 yr^{-1} in FFICT4.2 due to the shift from more water-intensive primary energy sources (e.g. crude oil) to less water-intensive options such as mining production and natural gas) in 2095, and electricity water withdrawals may increase (or decrease) from 535 km^3 yr^{-1} in 2005 to 755 km^3 yr^{-1} in the UCT4.2 scenario (or to 466 km^3 yr^{-1} in FFICT7.7) in 2095. The large drop in electric-sector water withdrawals around mid-century arises due to the assumed long-term phase-out of once-through flow cooling systems, which are characterized by high water withdrawal rates, in favor of lower-withdrawal wet towers, cooling ponds, and dry cooling systems. Manufacturing water withdrawals increase from 209 km^3 yr^{-1} in 2005 to 749–934 km^3 yr^{-1} (UCT scenarios),

Full Screen / Esc

Printer-friendly Version

Interactive Discussion

and to 820–895 km^3 yr^{-1} (FFICT scenarios) in 2095. In total, global water withdrawals increase from 3710 km^3 yr^{-1} in 2005 to 12 533–13 010 km^3 yr^{-1} (UCT scenarios), and to 13 935–25 357 km^3 yr^{-1} (FFICT scenarios) in 2095, thus, suggesting worsening water scarcity in the future.

Figure 8 shows the relative change in total water withdrawals for each of the demand sectors between the baseline scenario and each of the six climate policy scenarios. The effect of climate change mitigation policies on the estimated water withdrawals varies across water demand sectors. When comparing the results of the policy scenarios to the baseline scenario, the projected changes in biomass water demand range between −53 % to 100 % in 2050 and −59 % to 1317 % in 2095. With more stringent FFICT policies (i.e. lower mitigation targets, e.g. 4.2 W m^{-2}), biomass water demand increases substantially, and it generally decreases with more stringent UCT policies. As compared to biomass, the sensitivity of crop water withdrawals to climate policy is much less evident and only ranges between 0–4 % in 2050 and −3 % to 4 % in 2095. The effect of climate policy on livestock water withdrawals (as compared to the baseline scenario) range between 0–14 % in 2050 and 0–38 % in 2095, with policy scenarios projecting lower demands and with larger reductions associated with more stringent policies; i.e. the largest drop in livestock water demands are under the UCT4.2 and FFICT4.2 scenarios. More stringent climate policies cause also greater reductions in primary energy water demands, however, with FFICT scenarios projecting lower demands than their equivalent UCT scenarios. The effect climate policy on electricity and manufacturing water withdrawals (as compared to the baseline scenario) range between −31 % to −3 % in 2050 and −14 to 39 % in 2095, and between −16 % to −1 % in 2050 and −29 to −11 % in 2095, respectively. In total, the attributed change in global water withdrawals from the policy scenarios range between −2 % and 2 % in 2050 and −6 % and 90 % in 2095. Thus, depending on the adopted policy type and target, climate change mitigation policies could either increase or decrease future global water withdrawals, an effect that becomes increasingly apparent especially during the second half of the century.

Printer-friendly Version

Interactive Discussion

Figure 9 shows the distribution of global water withdrawals by sector for the baseline scenario and each of the climate change mitigation policies. Three main observations: (1) crop water demands remain the dominant source of water withdrawals over the whole century with the exception of the FFICT4.2 scenario, (2) the share of water withdrawals for electricity generations diminishes over time, and (3) the share biomass water withdrawals start to emerge strongly with the more stringent FFICT scenarios (e.g. FFICT5.5 and FFICT4.2). However, some of those changes prevail under the baseline scenario as well. The decreasing share for electricity water withdrawal is due to the assumed long-term phase-out of once-through flow cooling systems, and occurs in the baseline scenario. Figure 10 shows Piechart distributions of global water withdrawals by sector for the baseline scenario in years 2005 and 2095, and each of the climate change mitigation policies in year 2095. Similar to year 2005, all distributions show agriculture as the dominant source of withdrawals followed by industry, and then domestic use. However, with the more stringent policies, the share of industrial water demands slightly diminishes and becomes comparable to the domestic share for both UCT and FFICT scenarios. The proportion of biomass share increases most dramatically under the more stringent FFICT scenarios, making it an important competitor for future water demands and reducing the shares attributed to other sectors, especially other crops.

4.3 Water scarcity

To assess water scarcity at the grid and basin scales, all the sectoral water demand results are downscaled to $0.5° \times 0.5°$ following the methodology of the companion paper (Hejazi et al., 2013c). With projections of gridded water demand and supply results, global maps of water scarcity are produced for the years 2005 and 2095. Figure 11 shows the gridded global maps of water scarcity for the baseline and the six policy scenarios in the year 2095. Recall, a water scarcity index value of 0.4 or higher (WSI $\geq$ 0.4) denotes severe scarcity, (0.2 $\leq$ WSI < 0.4) denotes moderate scarcity, (0.1 $\leq$ WSI < 0.2) denotes low scarcity and (WSI < 0.1) denotes no scarcity, or abundant water resources as compared with demands. Generally, the gridded global

water scarcity map is spatially consistent across all scenarios with regions in eastern China, Northern India, and the Middle East projected to experience extreme scarcity conditions in 2095. Since it is not clearly apparent from Fig. 11 how water scarcity has changed spatially over time or due to each of the climate policies, Fig. 12 shows the change in water scarcity index between 2095 and 2005, and Fig. 13 shows the departure of each of the six policy scenarios from the baseline scenario in year 2095.

Generally, in 2095 more regions experience similar or elevated water scarcity conditions (Fig. 12). More specifically, regions that are experiencing some level of scarcity are projected to experience even more scarcity primarily due to mounting demands and changes in water availability in various regions. The largest increases in scarcity over the 21st century include regions in eastern China, India, Western Europe, and the Middle East. Some of that change is attributed to the large increase in population and income effect in these regions under the adopted socioeconomic assumptions for all the scenarios. Comparing across policies, Fig. 13 shows that the policy-caused anomaly from the baseline scenario (no climate policy) in year 2095 is spatially heterogeneous and depends on both the policy type (UCT vs., FFICT) and stringency level (e.g. 7.7, 5.5, and 4.2 W m^{-2}). As shown in Fig. 8, compared to the baseline scenario, the global water demand could decrease by up to 5.9 % in 2095 under the most stringent UCT policy (UCT4.2), or increase by up to 90 % under the most stringent FFICT policy (FFICT4.2). Thus, when distributing that global result spatially (Fig. 13), the effects of climate policy propagate differently in different regions due to land use and energy choices in these regions governing water demands. Also the spatial variation is confounded by regional differences in the impact of climate change on water availability. Thus, there are regions that are projected to see more scarcity even though globally there will be less water demanded than the baseline scenario under the UCT scenarios. For example, regions in central Asia and western United States will experience more scarcity due to UCT climate policies while other regions will experience less scarcity, such as Africa, eastern Europe, and eastern United States. The reasons are complex and likely dependent on several interdependent factors, such as: energy and

land use choices that are spatially heterogeneous (e.g. policy-induced shifts in favor of a particular crop that is grown in particular regions causing higher water demands), the spatial heterogeneity of climate change effects on regional hydrology and water availability, changes in technological progress in different regions, variations in socioeconomic drivers, and so on. When the results are varied within a GCAM region, such as the United States, then the likely factor is variability in the agricultural sector water demands since those are modeled at the AEZ scale (e.g. there are 10 AEZs in the United States) and changes in water availability (e.g. GWAM's representation includes many grid cells in the United States). Under the FFICT scenarios, the spatial coverage is more homogeneous mainly because water demands for biomass production dominate these scenarios. Under the FFICT climate policy scenarios as compared to the baseline scenario, most regions will experience some increase of water scarcity. However, noting the scale difference between Figs. 12 and 13, it is apparent that projected increases in water scarcity between 2095 and 2005 are much larger than the difference between policy and no policy scenarios.

Aggregating water scarcity globally, Fig. 14a, b shows the likely shifts to the cumulative density function (cdf) of the fraction of global population living under different levels of scarcity (WSI) at the grid and basin scales, respectively. Comparing between 2095 and 2005 under the baseline scenario, the cdf curve shifts to left denoting exacerbated water scarcity conditions and higher fraction of global population living under water stress. The thin lines reflect the uncertainty corresponding to any single climate model of the four GCMs instead of the ensemble mean of total annual water availability. The cdf in 2095 shifts slightly to the right under the UCT4.2 scenario and much further to the left under the FFICT4.2 scenarios. Thus, globally on average, UCT climate policies moderately alleviate water scarcity conditions and FFICT climate policies induce the opposite and more pronounced effect on water scarcity. Figure 14 shows the fraction of global population living in grid cells that are classified as severe scarcity conditions (WSI $\geq$ 0.4) for the baseline scenario and the six policy scenarios in years 2050 (Fig. 15a) and 2095 (Fig. 15b). The dashed bars reflect the level of uncertainty if

a single GCM is used instead of the ensemble of four GCMs to compute water availability for each grid. Global populations living in grid cells (basins) under severe water stress conditions increase from 42 % (29 %) in year 2005 to about 56 % (56 %) in year 2050 and to 66 % (64 %) in year 2095 in the baseline scenario; i.e. more than half of the world population will live under severe scarcity conditions in year 2050. The 2095 values drop to about 64 % (57 %) under the various UCT scenarios with no observable direction of change due to more stringent UCT climate policies. In contrast, the percentage of the global population living under severe water stress conditions in 2095 increases with more stringent FFICT policies, rising from 66 % (64 %) under the baseline scenario to 72 % (77 %) under the FFICT4.2 scenario. Table 1 summarizes the proportion of global population living under each water scarcity category for the baseline scenarios and the six policy scenarios in years 2050 and 2095.

When compared to previous water scarcity estimates from the literature for current population experiencing scarcity conditions (1995–2000), our estimates in year 2005 generally fall within the documented range. Figure 16 shows a comparison of the estimated percentage of the global population living in grids (Fig. 16a) and basins (Fig. 16b), and under different thresholds of water scarcity conditions with previous estimates from the literature (Wada et al., 2011 and baselines therein; Arnell et al., 2002, 2011; Alcamo et al., 2007). The spread in our results reflect the uncertainty arising from relying on each of the GCMs separately and the various climate policies, both singly and in tandem. Although we found that variation in water availability due to different emission policies is less than those attributed to using different GCMs (Fig. 4), Fig. 16 shows the opposite in terms of estimates of the global population living under severe water scarcity in 2095, i.e. more uncertainty from the various emission scenarios (policy scenarios) than from those attributed to using different GCMs, thus, signifying that changes in water demand are dominating changes in water supply. This result is consistent with the finding of Vörösmarty et al. (2000) that population growth plays a larger role in water scarcity than climate change in 2025. However, comparing the relative contributions of climate change, climate mitigation policies, and socioeconomic drivers

Title Page

Abstract | Introduction

Conclusions | References

Tables | Figures

◀ | ▶

◀ | ▶

Back | Close

Full Screen / Esc

Printer-friendly Version

Interactive Discussion

on water scarcity far longer in the future is yet to be tackled. Figure 17 shows a comparison between the grid- and basin-scale results along with other estimates from the literature for severely water stressed global population. Grid-based estimates overestimate scarcity as compared to basin-based estimates but that difference diminishes as scarcity increases. Note that the wide range of historical results (Figs. 16 and 17) signifies the wide level of uncertainty in such estimates. Uncertainty can arise from the method of estimating total water availability, projecting water demand, selecting spatial and temporal scales for the water scarcity calculations, and to downscaling demands to the appropriate scale. Future research should quantify the relative effect of those sources of uncertainties on water scarcity. Also, in this study we assume static population density maps; accounting for the diffusion of population over time is important to improve the realism of our findings.

Under the most stringent FFICT scenario (FFICT4.2), global water withdrawals increase from $3710\,km^3\,yr^{-1}$ in 2005 to $25\,357\,km^3\,yr^{-1}$ in 2095. But, is this quantity even physically feasible? Postel et al. (1996) estimated that out of the of the $40\,700\,km^3\,yr^{-1}$ global mean annual runoff volume, $7774\,km^3\,yr^{-1}$ is inaccessible for human use, $20\,426\,km^3\,yr^{-1}$ is uncaptured floodwater that flows directly to the world oceans, and only the remaining $12\,500\,km^3\,yr^{-1}$ is geographically and temporally accessible runoff, of which $2350\,km^3\,yr^{-1}$ is needed for instream water uses. Thus, humans' access to renewable water is approximately $10\,150\,km^3\,yr^{-1}$. Although this quantity may have increased over the past two decades with new reservoir storage capacity especially in developing regions, Postel's analysis suggests that all scenarios including the baseline scenario are potentially infeasible in the second half of the century. Recall that global water withdrawals range between 8843–$9276\,km^3\,yr^{-1}$ in 2050 and between $12\,533$–$25\,357\,km^3\,yr^{-1}$ in 2095. This also highlights some of the limitation of the model to represent the feedback from water supply and demand imbalances on human choices with regard to their diets, energy use, and prevailing technologies. Furthermore, in all the scenarios, the prevalence of water technologies (e.g. cooling system, irrigation efficiency) is exogenously input in the model, however, the likely strong competition for

water among the competing users and the mounting scarcity over time could cause differences in the evolution of certain technologies from how they are assumed to function in this framework. Thus, a market-based or an allocation-based approach is necessary to permit the modeling framework to choose endogenously among various water technologies instead of being exogenously fed in the model. Other advances to the framework can focus on the impact of warming on yield and crop water requirements, the effect of CO_2 fertilization on crop water use efficiency, and the effect of elevating water temperatures in streams on cooling efficiencies, which are not accounted for in this study. Instream water requirements for ecosystems and recreational and navigational purposes are also not accounted for as part of the global total demand and will need to be included in the future.

5 Conclusions

To quantify changes in future water scarcity, estimates of water availability from the new gridded water-balance global hydrologic model (GWAM) are compared with global water demands as modeled in GCAM. The six water demand sectors in GCAM (irrigation, livestock, domestic, electricity generation, primary energy production, and manufacturing) provide the total annual water demand divided by sector, subsector, technology, and region that are associated with any GCAM reference or policy stabilization scenario. Six policy scenarios (two types and three targets of radiative forcings) are simulated in GCAM along with the associated water demands and supply projections, and estimates are made of their impacts on water scarcity and thus the populations facing more or less water scarcity conditions. The results indicate that water scarcity shifts differently with the increasing stringency of the adopted climate change mitigation policies in term of emission targets. When compared to a baseline scenario (no climate policy), water scarcity declines under a UCT mitigation policy while increases with a FFICT mitigation scenario by the year 2095, mainly due to variations in prevailing bioenergy productions. Under the UCT scenario, although with population growth

coupled with increasing energy and food demands, water scarcity is likely to increase driven by higher water demands, when compared to the reference scenario, less water scarcity is projected on a global average but with spatial variations. For the FFICT scenarios, more scarcity is projected with more stringent climate policies. Thus, depending on the adopted policy type and stringency level, climate mitigation could lead to more or less water scarcity. More effort is needed to characterize the sources of uncertainty in water scarcity estimates, which could arise from several sources, including the hydrologic model, demand representation, socioeconomic and technological change assumptions, downscaling algorithms, population growth dynamics, among other factors.

References

Alcamo, J. and Henrichs, T.: Critical regions: a model-based estimation of world water resources sensitive to global changes, Aquat. Sci., 64, 352–362, doi:10.1007/pl00012591, 2002.

Alcamo, J., Döll, P., Henrichs, T., Kaspar, F., Lehner, B., Rösch, T., and Siebert, S.: Global estimates of water withdrawals and availability under current and future "business-as-usual" conditions, Hydrol. Sci. J., 48, 339–348, doi:10.1623/hysj.48.3.339.45278, 2003.

Alcamo, J., Flörke, M., and Marker, M.: Future long-term changes in global water resources driven by socio-economic and climatic changes, Hydrol. Sci. J., 52, 247–275, doi:10.1623/hysj.52.2.247, 2007.

Arnell, N.: Climate change and global water resources: SRES emissions and socio-economic scenarios, Global Environ. Change, 14, 31–52, doi:10.1016/j.gloenvcha.2003.10.006, 2004.

Arnell, N., van Vuuren, D., and Isaac, M.: The implications of climate policy for the impacts of climate change on global water resources, Global Environ. Chang., 21, 592–603, doi:10.1016/j.gloenvcha.2011.01.015, 2011.

Berndes, G.: Bioenergy and water – the implications of large-scale bioenergy production for water use and supply, Global Environ. Chang., 12, 253–271, doi:10.1016/s0959-3780(02)00040-7, 2002.

Brendes, G.: Water Demand for Global Bioenergy Production: Trends, Risks and Opportunities, WBGU, Berlin, 2008.

Brenkert, M., Smith, S., Kim, S., and Pitcher, H.: Model documentation for the MiniCAM, Pacific Northwest National Laboratory, Richland, Washington, 2003.

Brown, A. and Matlock, M.: A Review of Water Scarcity Indices and Methodologies: the Sustainability Consortium, University of Arkansas, Fayetteville, Arkansas, 2011.

Cabré, M., Solman, S., and Nuñez, M.: Creating regional climate change scenarios over southern South America for the 2020's and 2050's using the pattern scaling technique: validity and limitations, Clim. Change, 98, 449–469, doi:10.1007/s10584-009-9737-5, 2010.

Chaturvedi, V., Hejazi, M., Edmonds, J., Clarke, L., Kyle, P., Davies, E., Wise, M., and Calvin, K.: Climate policy implications for agricultural water demand, Clim. Policy, in review, 2013.

Clarke, L., Lurz, J., Wise, M., Edmonds, J., Kim, S., Pitcher, H., and Smith, S.: Model Documentation for the MiniCAM Climate Change Science Program Stabilization Scenarios, Pacific Northwest National Laboratory Richland, WA, Richland, Washington, USA, 2007.

Davies, E., Kyle, P., and Edmonds, J.: An integrated assessment of global and regional water demands for electricity generation to 2095, Adv. Water Resour., 52, 296–313, 2013.

Edmonds, J. and Reilly, J.: Global Energy: Assessing the Future, Oxford University Press, New York, 1985.

Falkenmark, M.: Forward to the future: a conceptual framework for water dependence, Ambio, 28, 356–361, 1999.

Gerbens-Leenes, P., Hoekstra, A., and van der Meer, T.: The water footprint of energy from biomass: a quantitative assessment and consequences of an increasing share of bio-energy in energy supply, Ecol. Econ., 68, 1052–1060, doi:10.1016/j.ecolecon.2008.07.013, 2009.

Hejazi, M., Edmonds, J., Chaturvedi, V., Davies, E., and Eom, J.: Scenarios of global municipal water use demand projections over the 21st century, Hydrol. Sci. J., accepted, 2013a.

Hejazi, M., Edmonds, J., Clarke, L., Kyle, P., Chaturvedi, V., Davies, E., Wise, M., Patel, P., Eom, J., and Calvin, K.: Long-term global water use projections using six socioeconomic

scenarios in an integrated assessment modeling framework, Technol. Forecast. Soc., in re-
view, 2013b.

Hejazi, M. I., Edmonds, J., Clarke, L., Kyle, P., Davies, E., Chaturvedi, V., Wise, M., Patel, P.,
Eom, J., and Calvin, K.: Integrated assessment of global water scarcity over the 21st century
5 – Part 1: Global water supply and demand under extreme radiative forcing, Hydrol. Earth
Syst. Sci. Discuss., 10, 3327–3381, doi:10.5194/hessd-10-3327-2013, 2013c.

Jackson, R. B., Carpenter, S. R., Dahm, C. N., McKnight, D. M., Naiman, R. J., Postel, S. L., and
Running, S. W.: Water in a changing world, Ecol. Appl., 11, 1027–1045, doi:10.1890/1051-
0761(2001)011[1027:wiacw]2.0.co;2, 2001.

10 Kim, S., Edmonds, J., Lurz, J., Smith, S., and Wise, M.: The object-oriented energy cli-
mate technology systems (ObjECTS) framework and hybrid modeling of transportation
in the MiniCAM long-term, global integrated assessment model, Energ. J., 27, 63–92,
doi:10.5547/ISSN0195-6574-EJ-VolSI2006-NoSI2-4, 2006.

Milly, P., Dunne, K., and Vecchia, A.: Global pattern of trends in streamflow and water availability
15 in a changing climate, Nature, 438, 347–350, 2005.

Mitchell, T. D. and Jones, P. D.: An improved method of constructing a database of monthly
climate observations and associated high-resolution grids, Int. J. Climatol., 25, 693–712,
doi:10.1002/joc.1181, 2005.

Postel, S. L., Daily, G. C., and Ehrlich, P. R.: Human appropriation of renewable fresh water,
20 Science, 271, 785–788, doi:10.1126/science.271.5250.785, 1996.

Raskin, P., Gleick, P., Kirshen, P., Pontius, G., and Strzepek, K.: Water Futures: Assessment of
Long-range Patterns and Prospects, Stockholm Environment Institute, Stockholm, Sweden,
1997.

Shen, Y., Oki, T., Utsumi, N., Kanae, S., and Hanasaki, N.: Projection of future world water
25 resources under SRES scenarios: water withdrawal/Projection des ressources en eau mon-
diales futures selon les scénarios du RSSE: prélèvement d'eau, Hydrol. Sci. J., 53, 11–33,
doi:10.1623/hysj.53.1.11, 2008.

SRES: Special Report on Emissions Scenarios: a special report of Working Group III of the In-
tergovernmental Panel on Climate Change, edited by: Nakićenović, N. and Swart, R., Cam-
30 bridge University Press, Cambridge, ENGLAND, UK, 2000.

Varghese, S.: Biofuels and global water challenges, Institute for Agriculture Trade and Policy,
Minneapolis, Minnesota, USA, 2007.

**Climate change
mitigation policies**

M. I. Hejazi et al.

Title Page

Abstract	Introduction
Conclusions	References
Tables	Figures

Back | Close

Full Screen / Esc

Printer-friendly Version

Interactive Discussion

Vörösmarty, C., Green, P., Salisbury, J., and Lammers, R.: Global water resources: vulnerability from climate change and population growth, Science, 289, 284–288, doi:10.1126/science.289.5477.284, 2000.

Wada, Y., van Beek, L., Viviroli, D., Dürr, H., Weingartner, R., and Bierkens, M.: Global monthly water stress: 2. Water demand and severity of water stress, Water Resour. Res., 47, W07518, doi:10.1029/2010wr009792, 2011.

Wise, M., Calvin, K., Thomson, A., Clarke, L., Bond-Lamberty, B., Sands, R., Smith, S. J., Janetos, A., and Edmonds, J.: Implications of limiting CO_2 concentrations for land use and energy, Science, 324, 1183–1186, 2009.

Table 1. Water scarcity under different climate mitigation policies and tax regimes; scarcity is calculated at the grid-scale (basin-scale).

Time Period	Tax Regime	RF in 2095 (Wm^{-2})	No Stress	Low Stress	Moderate Stress	Severe Stress
2005			0.295 (0.277)	0.141 (0.211)	0.145 (0.224)	0.419 (0.289)
2050	Baseline	8.8	0.194 (0.108)	0.110 (0.148)	0.131 (0.180)	0.565 (0.564)
	UCT	7.7	0.200 (0.161)	0.113 (0.116)	0.128 (0.167)	0.560 (0.556)
	UCT	5.5	0.217 (0.183)	0.111 (0.104)	0.129 (0.199)	0.543 (0.514)
	UCT	4.2	0.227 (0.183)	0.113 (0.123)	0.126 (0.189)	0.534 (0.505)
	FFICT	7.7	0.194 (0.108)	0.110 (0.148)	0.131 (0.183)	0.566 (0.561)
	FFICT	5.5	0.198 (0.101)	0.112 (0.155)	0.130 (0.185)	0.561 (0.559)
	FFICT	4.2	0.200 (0.101)	0.113 (0.144)	0.129 (0.191)	0.558 (0.565)
2095	Baseline	8.8	0.123 (0.079)	0.089 (0.061)	0.125 (0.219)	0.664 (0.641)
	UCT	7.7	0.140 (0.101)	0.093 (0.140)	0.123 (0.143)	0.644 (0.616)
	UCT	5.5	0.150 (0.121)	0.092 (0.140)	0.119 (0.167)	0.639 (0.573)
	UCT	4.2	0.146 (0.127)	0.092 (0.123)	0.122 (0.138)	0.640 (0.612)
	FFICT	7.7	0.127 (0.074)	0.087 (0.062)	0.121 (0.183)	0.666 (0.681)
	FFICT	5.5	0.114 (0.064)	0.074 (0.045)	0.104 (0.133)	0.708 (0.758)
	FFICT	4.2	0.109 (0.056)	0.070 (0.047)	0.101 (0.127)	0.720 (0.770)
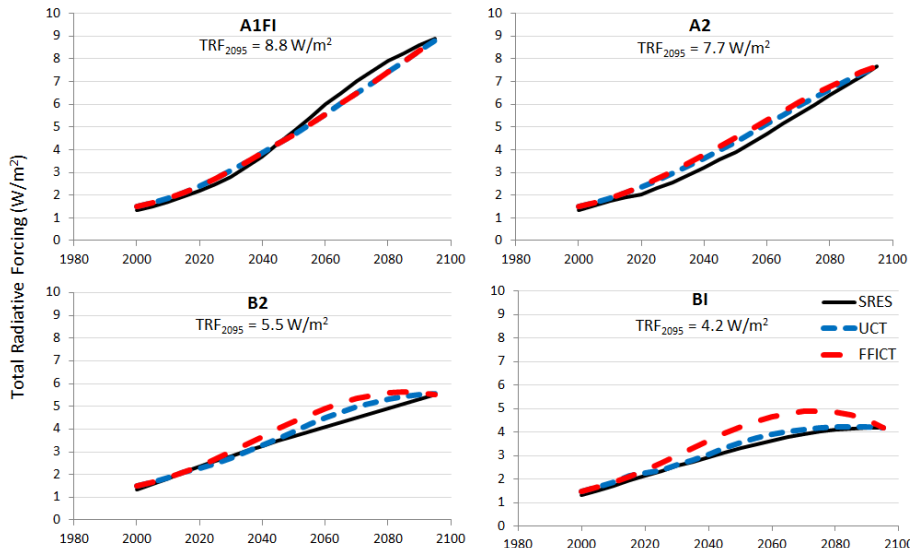
Fig. 1. Radiative forcing trajectories based on each of the four SRES emission scenarios (A1fi, A2, B2, and B1); blue and red dashed lines are GCAM equivalent simulations of the UCT and FFICT tax regimes to replicate SRES's emission pathways.
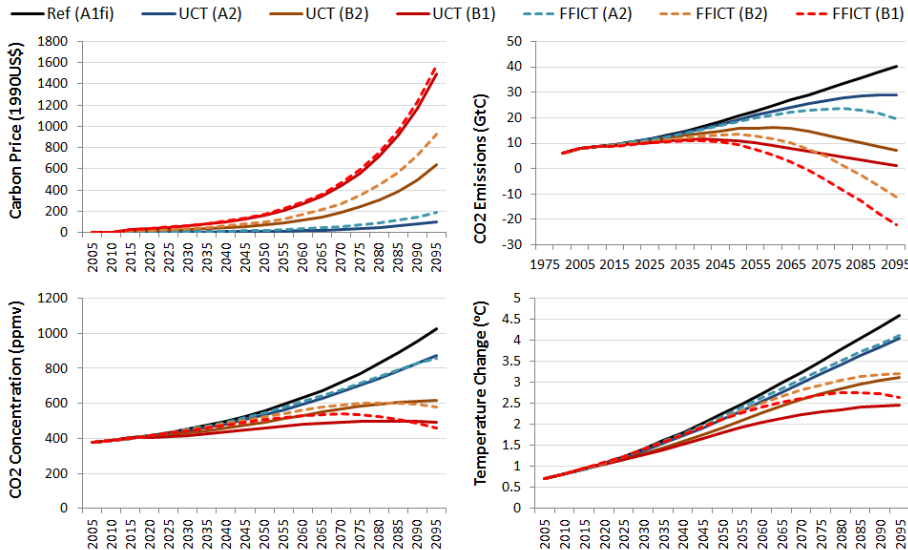
Fig. 2. The resulting carbon price, CO_2 emission and concentration, and mean global temperature change associated with both the UCT and FFICT tax regimes and all four emission scenarios (A1fi, A2, B2, and B1); the A1fi scenario (black solid line) reflects the no-climate policy scenario (baseline).
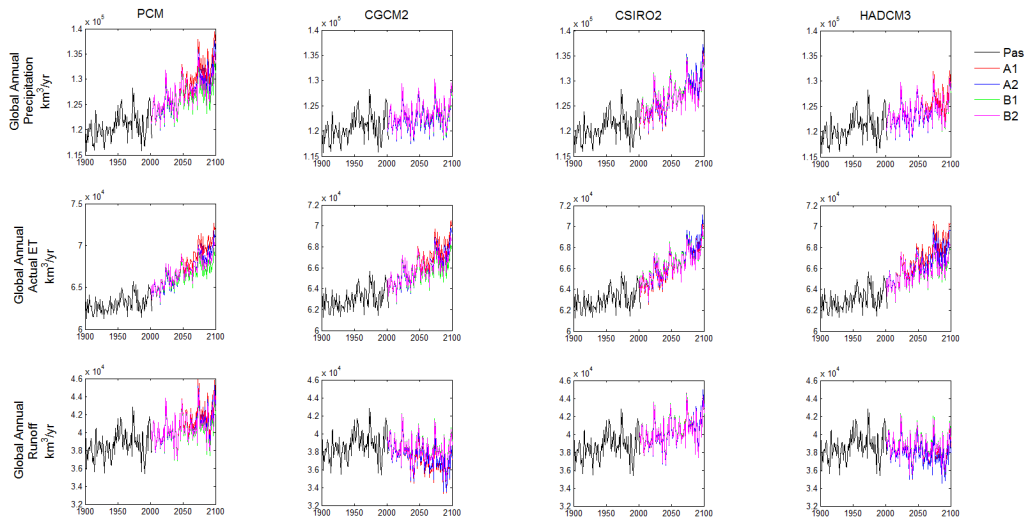
Fig. 3. Global annual precipitation, actual evapotranspiration, and runoff from 1901–2100; future values are from four GCMs (PCM, CGCM2, CSIRO2, and HADCM3) and for emission scenarios (A1fi, A2, B1, and B2).

Discussion Paper | Discussion Paper | Discussion Paper | Discussion Paper

HESSD

10, 3383–3425, 2013

Climate change mitigation policies

M. I. Hejazi et al.

Title Page

Abstract | Introduction

Conclusions | References

Tables | Figures

|◀ | ▶|

◀ | ▶

Back | Close

Full Screen / Esc

Printer-friendly Version

Interactive Discussion
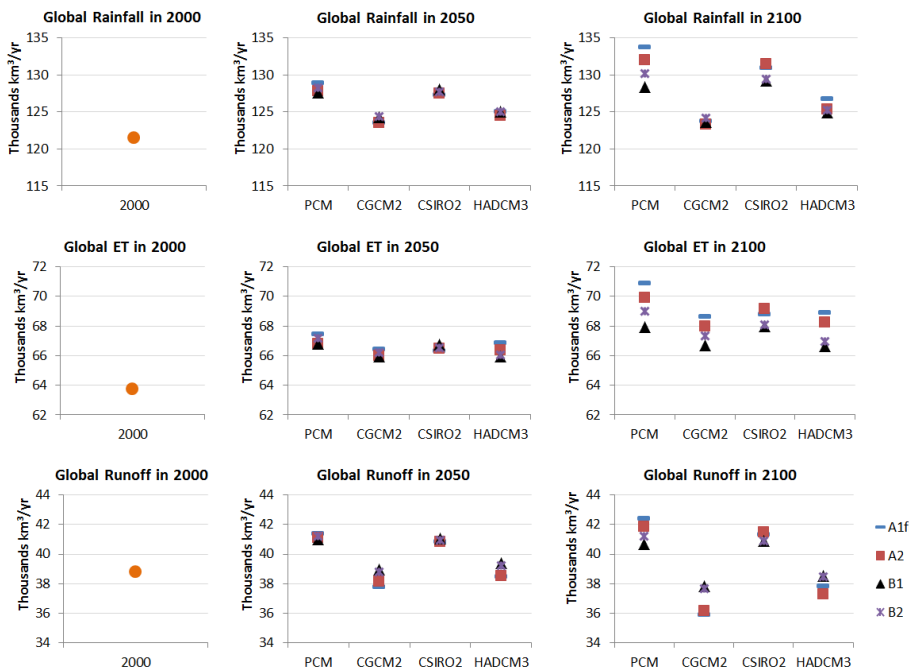
Fig. 4. Comparison of annual precipitation, actual ET, and runoff estimates across GCMs and emission scenarios in years 2000, 2050, and 2095; uncertainty across GCMs is larger than scenarios, and the uncertainty level increases with time, i.e. uncertainty is larger in 2100 than 2050.
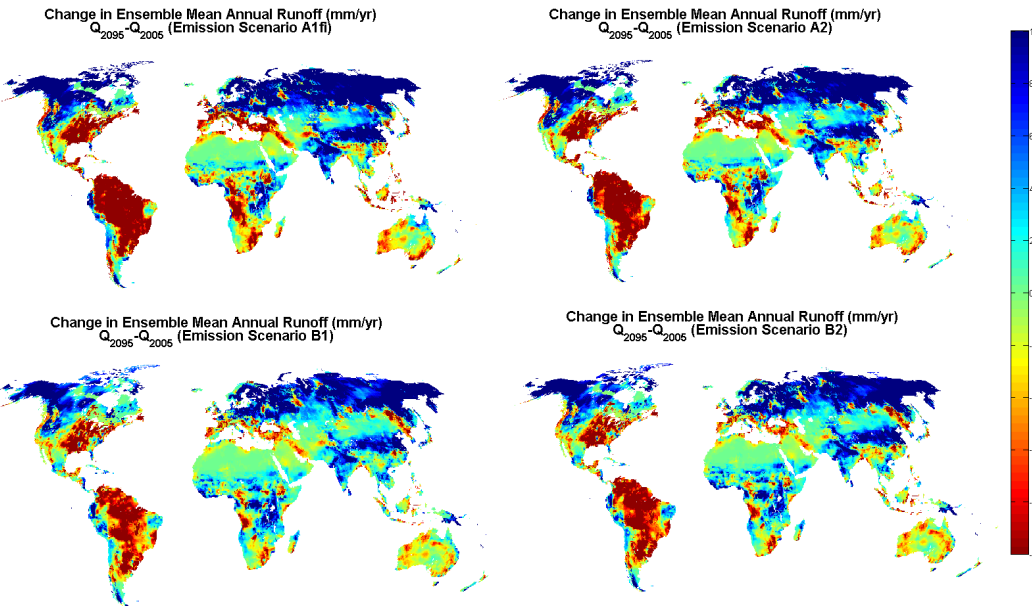
Fig. 5. Change in ensemble mean annual runoff between 2095 and 2005 for each of the four emission scenarios (A1fi, A2, B1, and B2).

Printer-friendly Version

Interactive Discussion
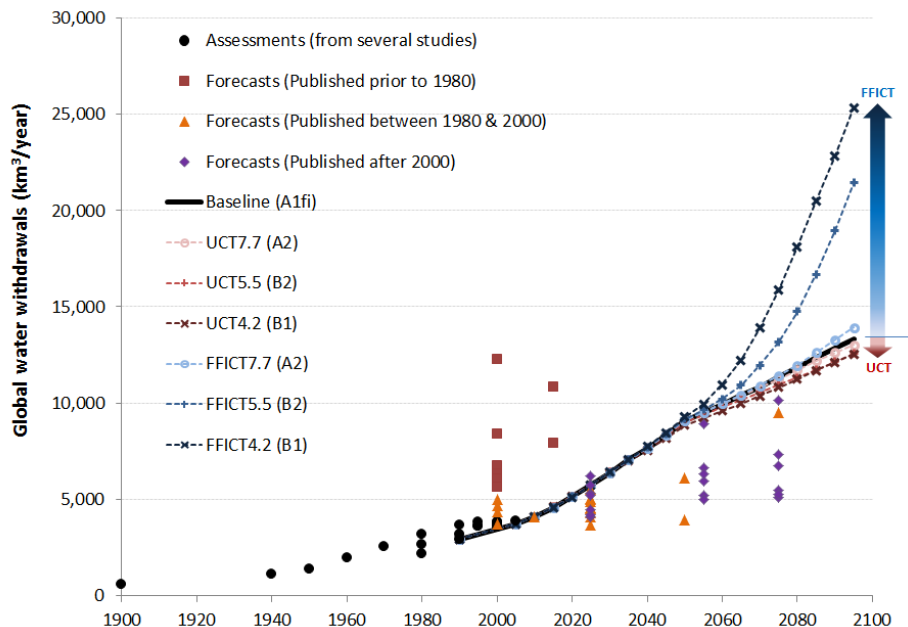
Fig. 6. Global water withdrawals for the baseline and the six policy scenarios in comparison to literature estimates of historical water use and other studies; sources: Gleick (2003, and references therein); Falkenmark and Rockström (2000); Alcamo et al. (2003a, b, 2007); Shiklomanov and Rodda (2003); Shen et al. (2008); Wada et al. (2011); and AQUASTAT (2011).
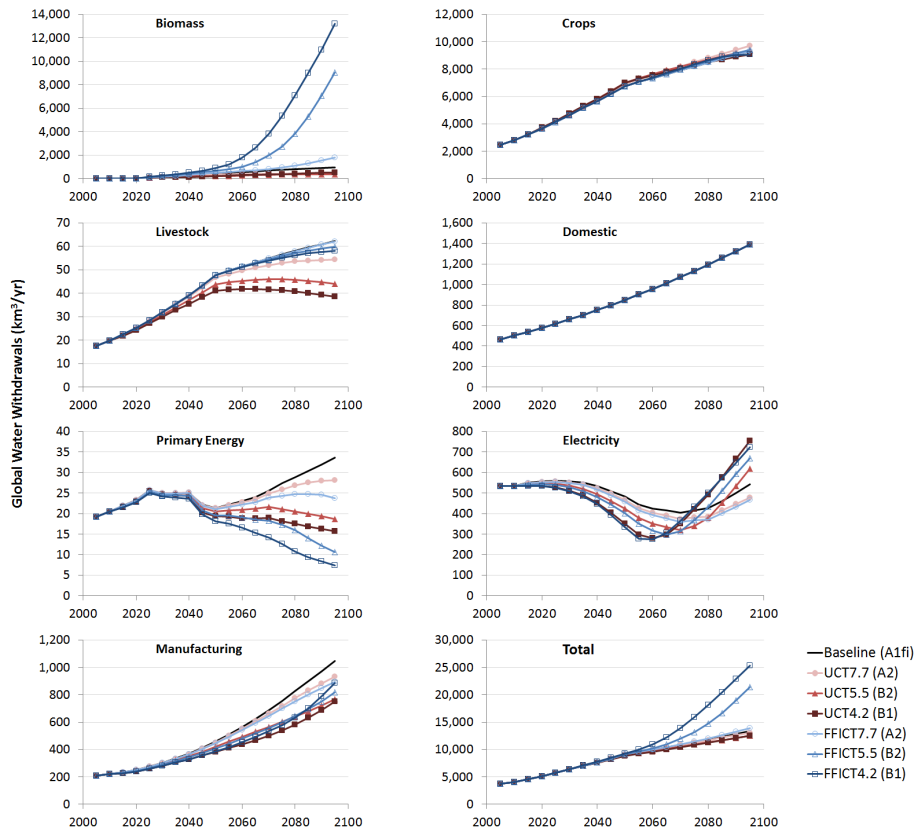
Fig. 7. GCAM's estimates of global water demands (withdrawals) for the baseline (A1fi) scenario (no climate policy) and the six climate change mitigation policy scenarios (UCT7.7 (A2), UCT5.5 (B2), UCT4.2 (B1), FFICT7.7 (A2), FFICT5.5 (B2), FFICT4.2 (B1)) for each of the water demand sectors.
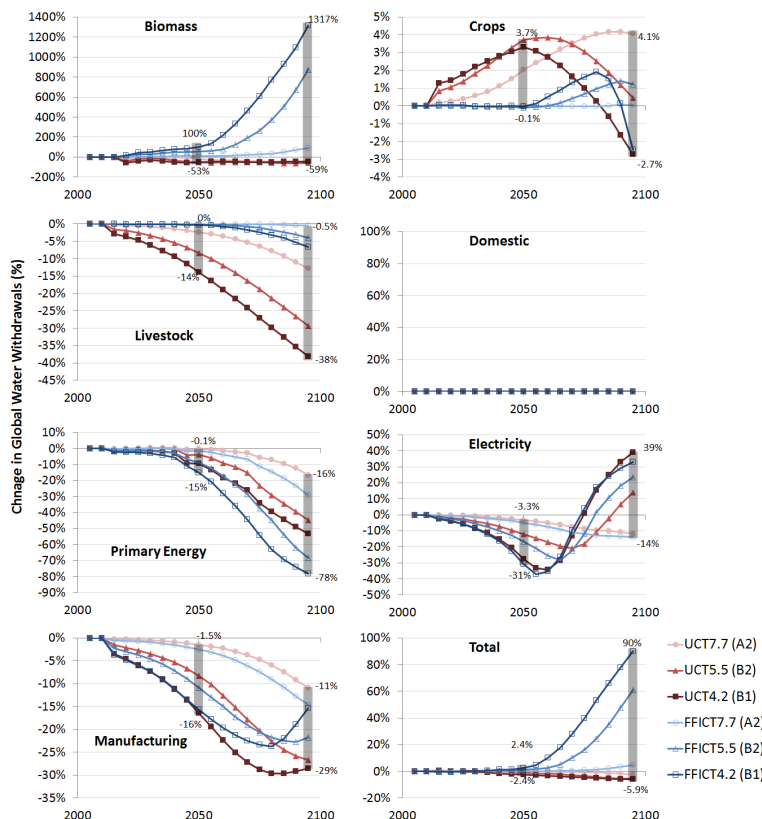
Fig. 8. Deviations in GCAM's estimates of global water withdrawals from the baseline (A1fi) scenario (no climate policy) for each of the six climate change mitigation policy scenarios (UCT7.7 (A2), UCT5.5 (B2), UCT4.2 (B1), FFICT7.7 (A2), FFICT5.5 (B2), FFICT4.2 (B1)) for each of the water demand sectors.
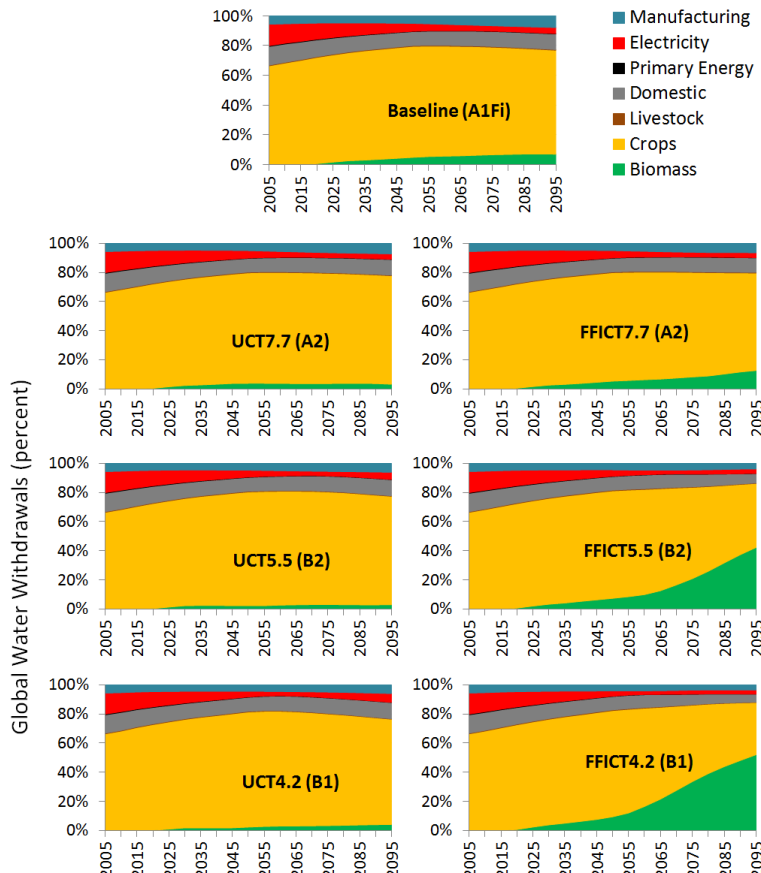
Fig. 9. GCAM's distribution of global water demands (withdrawals) by demand sector for the baseline scenario (no climate policy) and the six climate change mitigation policy scenarios.

Title Page

Abstract | Introduction

Conclusions | References

Tables | Figures

◄ | ►

◄ | ►

Back | Close

Full Screen / Esc

Printer-friendly Version

Interactive Discussion

Fig. 10. Piechart distributions of global water demands (withdrawals) by sector for the baseline scenario (A1fi) in years 2005 and 2095, and for each of the climate change mitigation policies (2 tax regimes (UCT & FFICT) × 3 emission scenarios (A2, B2, and B1)).

Title Page

Abstract | Introduction

Conclusions | References

Tables | Figures

◀ | ▶

◀ | ▶

Back | Close

Full Screen / Esc

Printer-friendly Version

Interactive Discussion
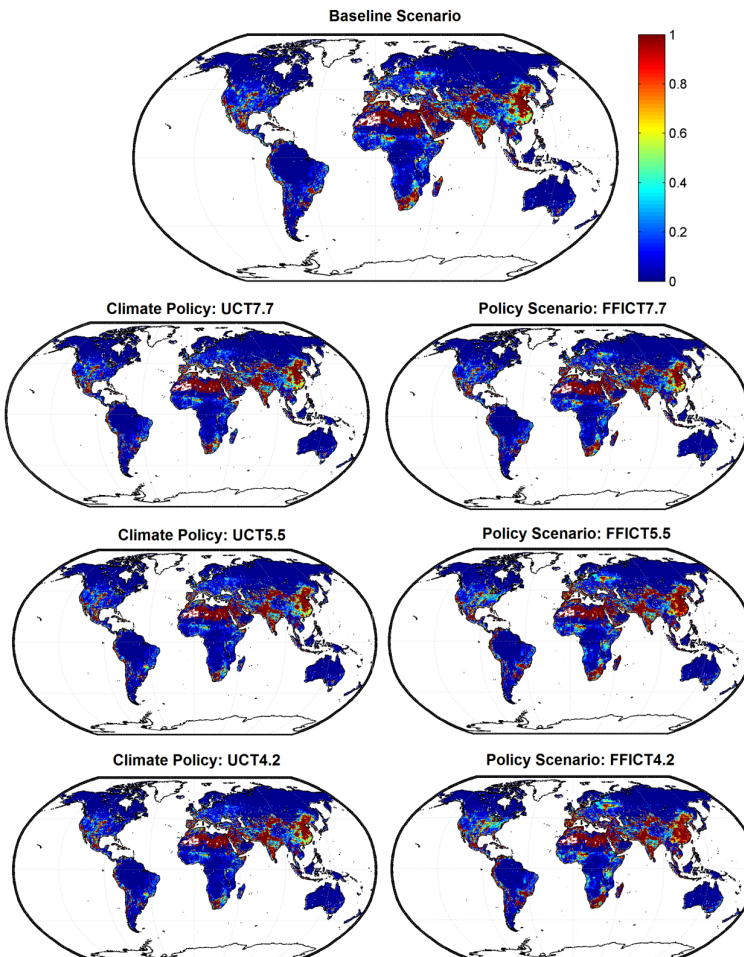
Fig. 11. GCAM's downscaled water scarcity results in year 2095 under each of the climate policies.

Title Page

Abstract | Introduction

Conclusions | References

Tables | Figures

◄ | ►►

◄ | ►

Back | Close

Full Screen / Esc

Printer-friendly Version

Interactive Discussion
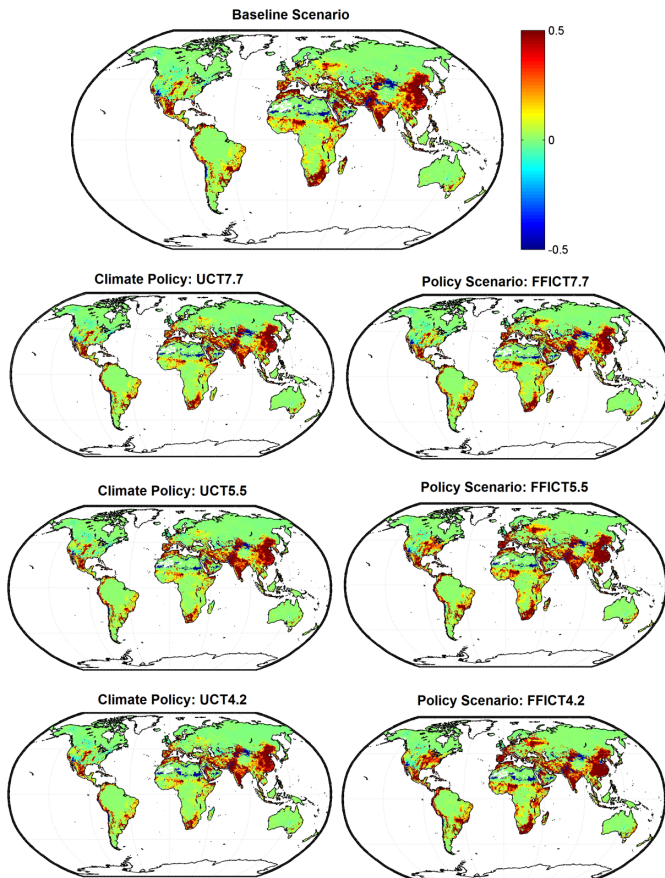
Fig. 12. Changes in water scarcity conditions from 2005 to 2095 different climate change mitigation policies; positive values (red) denote increased scarcity conditions in 2095 as compared to 2005.

Full Screen / Esc
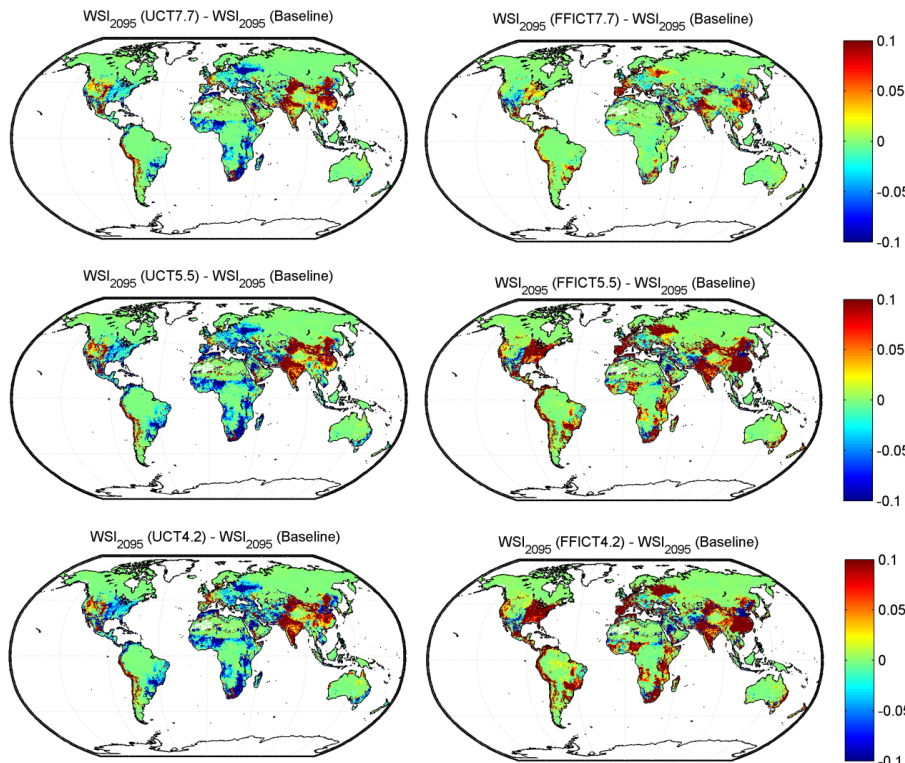
Fig. 13. The effect of climate change mitigation policies on the magnitude of the WSI; all six policy scenarios are compared to the baseline scenario (A1fi) in 2095.

Title Page

Abstract | Introduction

Conclusions | References

Tables | Figures

◄ | ►

◄ | ►

Back | Close

Full Screen / Esc

Printer-friendly Version

Interactive Discussion
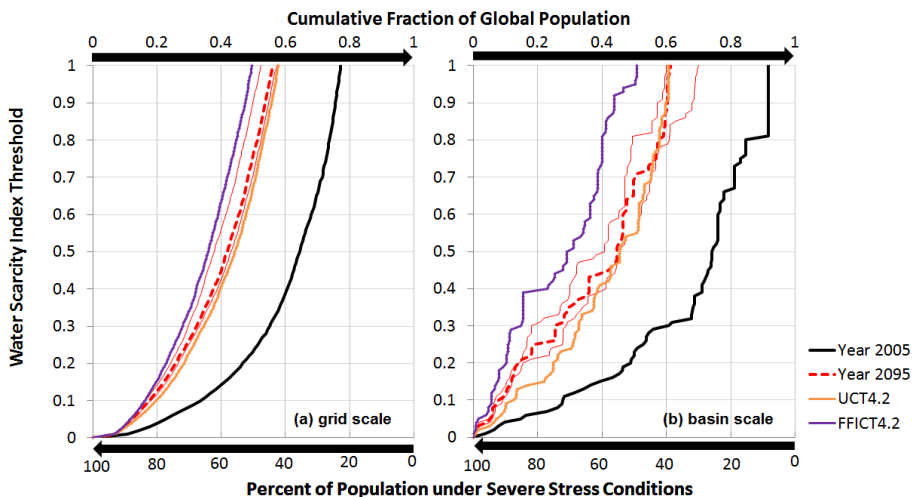
Fig. 14. Shifts to the cumulative probability density function of the fraction of global population living under different levels of scarcity (WSI); water scarcity is estimated at the grid **(a)** and basin **(b)** scales; the thin lines reflect the uncertainty corresponding to the any one of the four GCMs instead of the ensemble mean.
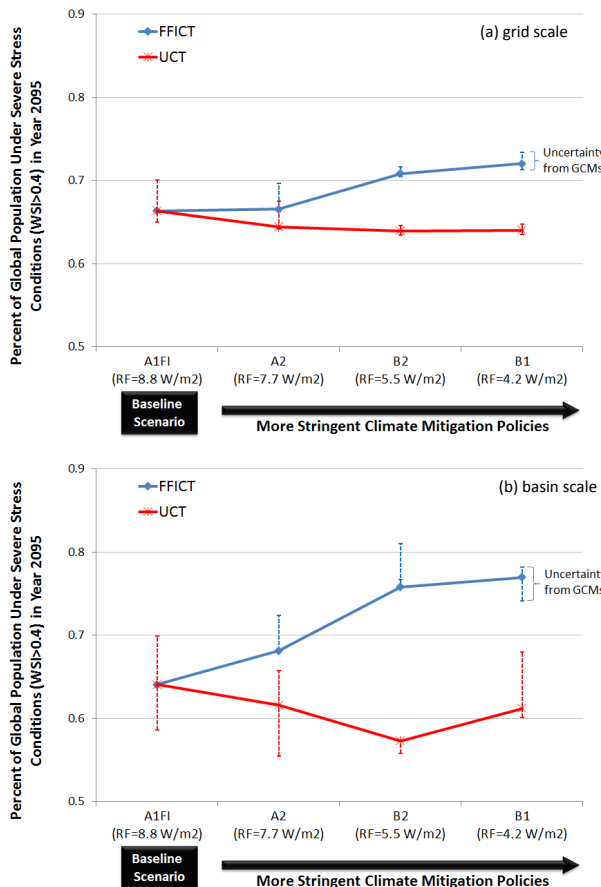
Fig. 15. percent of population living under severe water scarcity conditions in year 2095 under different climate policies and with increasing stringency; error bars reflect the level of uncertainty if a single GCM is used instead of the ensemble of four GCMs.
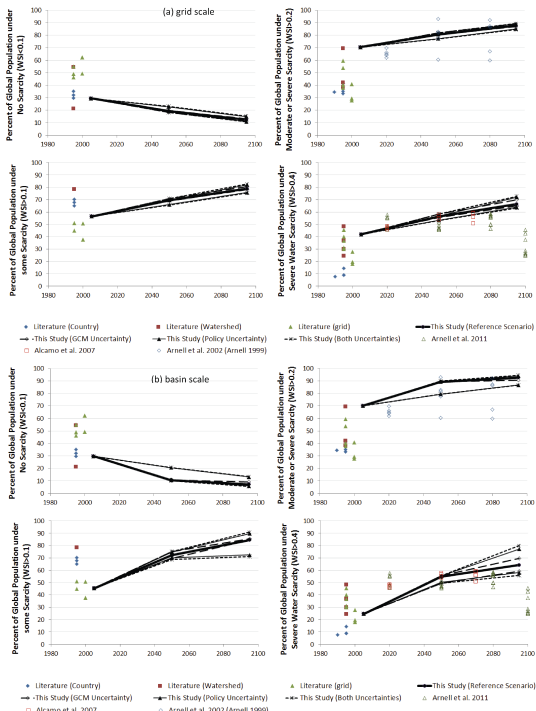
Fig. 16. Comparison of the estimated percent of global population living different thresholds of water scarcity conditions with previous estimates from the literature (Wada et al., 2011 and references therein; Arnell et al., 2002, 2011; Alcamo et al., 2007); the spread in our results reflect the uncertainty arising from relying on each of the GCMs separately and the various climate policies, both singly and in tandem; the shape denotes the spatial scale of estimating WSI (blue diamonds: country scale; red squares: watershed scale; and green triangles: grid scale); solid points reflect assessments of current or historical scarcity conditions; empty shapes denote projections in the future.
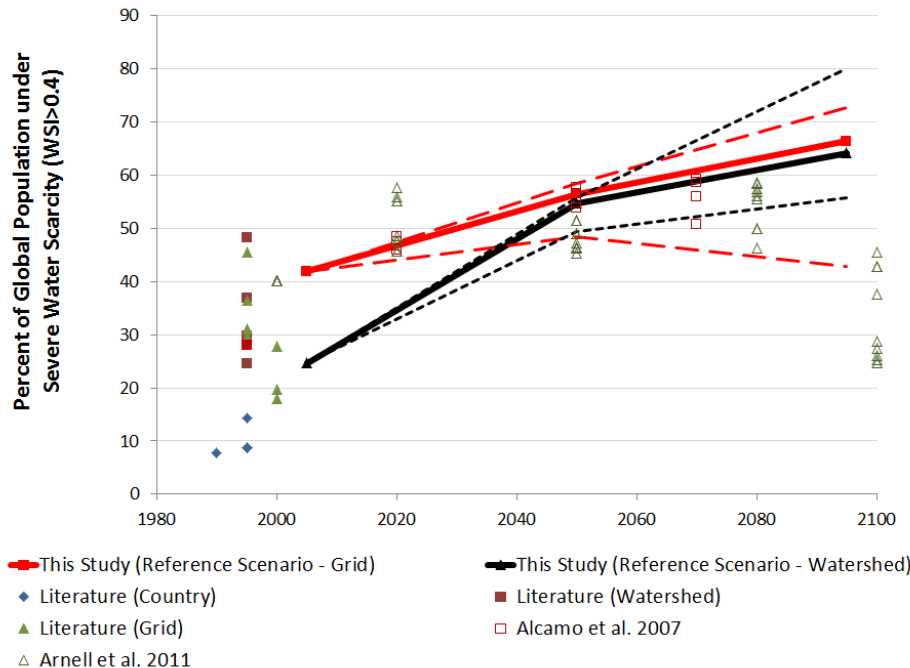
Fig. 17. Comparison of the estimated percent of global population under severe water stress in grid cells (black lines) and basin areas (red lines) along with previous estimates from the literature (Wada et al., 2011 and references therein; Arnell et al., 2002, 2011; Alcamo et al., 2007); the spread in our results reflect the uncertainty arising from relying on each of the GCMs separately and the various climate policies (dashed lines); the shape denotes the spatial scale of estimating WSI (blue diamonds: country scale; red squares: watershed scale; and green triangles: grid scale); solid points reflect assessments of current or historical scarcity conditions; empty shapes denote projections in the future.